

Cindy Yuen

Chem E 499

April 20<sup>th</sup>, 2008

Solved 2-D Parameters

## Introduction

The objective of this project is to characterize the degree of mixing and flow patterns in 2-D associated with varying Reynolds and Peclet numbers for a self circulating mixing chamber and then compare results with those observed in the paper, “Design of passive mixers utilizing microfluidic self-circulating in the mixing chamber.” In addition, 2 D and 3 D results were obtained for mixers in series. The variances of the 2D, 3D with slip conditions, and 3D with no slip will be compared to determine the validity of the results obtained for the 3D with slip and no slip.

## Device Modeled

The micro-fluidic device modeled is a self circulating mixing chamber from the paper, “Design of passive mixers utilizing microfluidic self-circulation in the mixing chamber,” by Yung-Chiang et al. In the paper, flow is injected into the channels and mixing chamber and then actuated back and forth by a pump, causing the flow to move back and forth through the mixer at any one given time. A schematic of this device is shown in Figure 1 where fluid enters at the device and flow circulation is divided into two parts. Part M is the main of the flow that is able to exit the device where part S is the self circulating part of the flow the remains within the chamber.

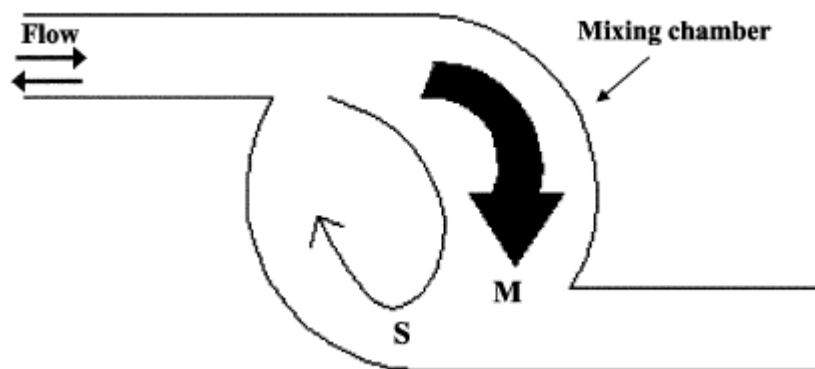


Figure 1: **Self Circulating Mixing Chamber.** *In the paper, fluid is actuated back and forth from through a single mixer, which why flow is depicted in both directions from the top. The M depicts the main flow that exits the mixer. S is the portion of flow that continues to recirculate in the mixer.*

According to the paper, the design of this microfluidic device was meant to improve mixing by increasing the contact area of the fluid by forming a free vortex, deemed the S portion of the flow. Modeling performed in the paper was done using CFD-ACE™ software which numerically predicts the flow field within the mixer by solving the Navier-Stokes and continuity equations. The Reynolds numbers modeled were in the range of 5 to 400, well within the laminar regime of flow. And in order to evaluate the mixing efficiency the percentage of mixing was calculated using the following equation.  $N_i$  represents the mole fraction of water at the sampling points in the mixer,  $N_{Equ}$  in the equilibrium fraction of water in the mixer,  $V_i$  is the volume of sampling points, and  $n$  is the number of sampling points. And the term in the denominator refers to inlet conditions [1].

$$\phi = \left( 1 - \frac{\sum_{i=1}^n |(N_i - N_{Equ}) V_i|}{\sum_{i=1}^n |(N_i - N_{Equ}) V_{i_o}|} \right) * 100\% \quad \text{Eqn.1}$$

The following results were those generated from the paper.

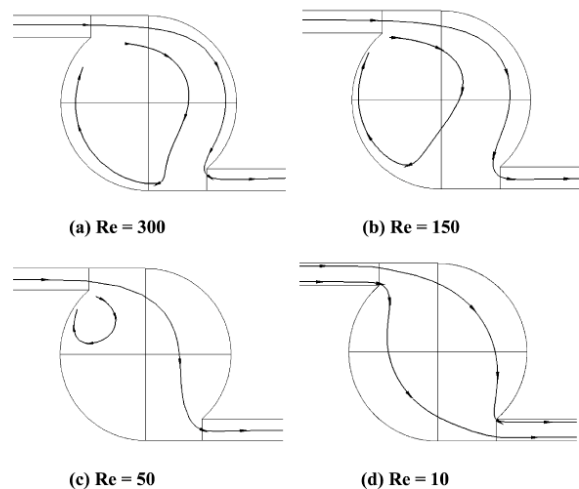


Fig. 8 Streamlines of flow in M1 at  $Re$  equals (a) 300, (b) 150, (c) 50 and (d) 10.

Figure 2. **Literature Reported Mixer Streamlines.** These are the streamline profile results in the paper generated from CFD-ACE™ software. Self-circulation of the fluid was reported at Reynolds numbers higher than the critical value of 20 [1].

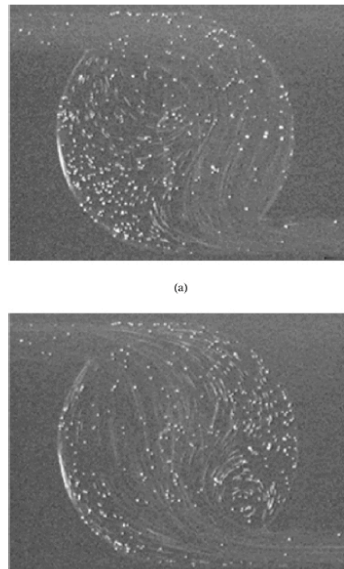


Figure 3. **Single Mixer Fluorescence Images.** These are the fluorescence images of fluid circulation within the mixer reported in the paper for  $Re=150$  for fluid moving from left to right and  $Re=50$  for fluid moving from right to left [1].

## Modeling Methods

In order to separately ascertain the mixing induced by the mixer under varying conditions, simulations were done in Comsol using the Navier-Stokes equations. However, unlike the paper additional modeling was done using diffusion and convection equations to ascertain mixing instead of using percentage of mixing mentioned above. Although flow was actuated back and forth in the mixer from the paper, as an approximation modeling for a single mixer was done in 2D under the assumption of steady state flows and diffusion for one modeling scenario. Subsequently the mixing was then characterized by varying the Reynolds and Peclet numbers while monitoring parameters such as mixing cup concentration, optical concentration, pressure, and concentration variances. Other modeling scenarios were also generated such as 2-D and 3-D modeling solutions for mixers in series. The following section provides the equations and definitions of the parameters mentioned.

## Theory

The following equations describe how each quantity is obtained by integrating concentration, velocity, or length over spatial boundary coordinates [3]. Eqn. 6 provides the dimensional form of the Navier-Stokes equation and the following equation is the non-dimensionalized form of the Navier-Stokes equation use for low Reynolds numbers up to 300 [2].

**C<sub>mixing cup</sub>**

$$c_{mixing\_cup} = \frac{\int c(x, y, z)v(x, y)dx dy}{\int_A v(x, y)dx dy} \quad \text{Eqn. 2}$$

**C<sub>variance</sub>**

$$c_{mixing\ variance} = \frac{\int (c(x, y, z) - c_{mixing\_cup})^2 v(x, y)dx dy}{\int_A v(x, y)dx dy} \quad \text{Eqn. 3}$$

**C<sub>optical</sub>**

$$c_{optical} = \int_0^L c(x, y, z)dy / \int_0^L dy \quad \text{Eqn. 4}$$

**C<sub>optical variance</sub>**

$$c_{optical\_variance} = \int_0^L (c(x, y, z) - c_{optical})^2 dy / \int_0^L dy \quad \text{Eqn. 5}$$

**P<sub>Avg</sub>**

$$P_{Avg} = \frac{\int P(x, y)dx dy}{\int dx dy} \quad \text{Eqn. 6}$$

**Dimensional Navier-Stokes Equation**

$$\rho \frac{\partial u}{\partial t} + \rho u * \nabla u = -\nabla p + \mu \nabla^2 u \quad \text{Eqn. 7}$$

**Non-dimensional Navier-Stokes Equation**

$$\text{Re} \frac{\partial u'}{\partial t'} + \text{Re} u' * \nabla' u' = -\nabla' p' + \nabla'^2 u' \quad \text{Eqn. 8}$$

$$\text{Re} = \frac{\rho u_s x_s}{\mu} \quad \text{Eqn. 9}$$

## Comsol 2-D & 3-D Input

For the initial modeling of concentration and flow, this device was first drawn in 2-D using Comsol Multiphysics using the same cross sectional area shown in Figure 1. The modeling options selected in the Comsol model navigator were incompressible flow using the Navier Stokes and diffusion and convection for steady state. The boundary conditions selected under the Navier Stokes equation were walls under the no slip condition, except for the inlet and outlet boundaries that were selected to have normal inflow velocity and pressure of 1 and 0 Pa. The boundary conditions selected for convection and diffusion were Insulation/Symmetry with no quantities specified for the walls of the mixers, while the inlet boundary condition is set to Concentration with the  $c_0$  quantity specified as  $(y < 1) * 1 + (y \geq 1) * 0$  and the exit was specified as Convective flux with no parameters specified. The same approach was again used for a series of four mixers in 2D modeling of mixers except the  $c_0$  quantity was set to  $(y < 3.5) * 1 + (y \geq 3.5) * 0$ .

For 3D modeling, the 2D version of the mixers in series was extruded and the Navier Stokes equation for incompressible flow and convection/diffusion modeling options for steady state were again selected. The boundary conditions for both sets of equations were set in the same manner as those for the 2D simulations.

## Results

First displaying the results of a single mixer in 2-D, the following figures are the streamlines and concentration gradients generated for varying Reynolds numbers.

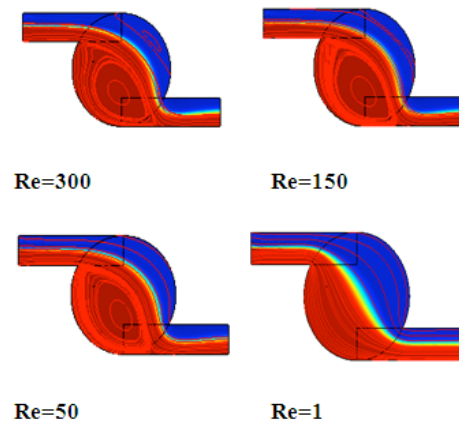


Figure 4. **Fluid Flows in a Single Mixer.** For the Reynolds numbers shown above with the Peclet number set to 1000, self circulation can be observed for Reynolds numbers excess of 50 whereas with lower Reynolds numbers no self circulation is observed as both fluids exit the mixer at the same time.

Re	Pe	_P	u	c_mixing	c_variance	x	c_optical	c_op_var
D'Less	D'Less	(Pa)	(m <sup>2</sup> /s)	(mol/(m*s))	(mol/(m*s))	(m <sup>2</sup> )	(mol/m)	(mol/m)
1	1000	69.68	0.958	0.531	0.169	4.5	0.518	0.196
10	1000	7.45	0.958	0.530	0.169	4.5	0.519	0.196
50	1000	2.31	0.958	0.526	0.167	4.5	0.505	0.197
150	1000	1.64	0.965	0.653	0.139	4.5	0.505	0.197
300	1000	1.54	0.965	0.750	0.106	4.5	0.505	0.197

Table 1: **Solved parameters for a Single 2D Mixer for Varying Reynolds Numbers.** This table contains the parameters obtained from varying the Reynolds number from 1 to 300 while maintaining the Peclet number constant at 1000. Mixing cup concentrations are observed to increase with respect to increasing Reynolds numbers. A slight decrease in corresponding mixing variances is also observed.

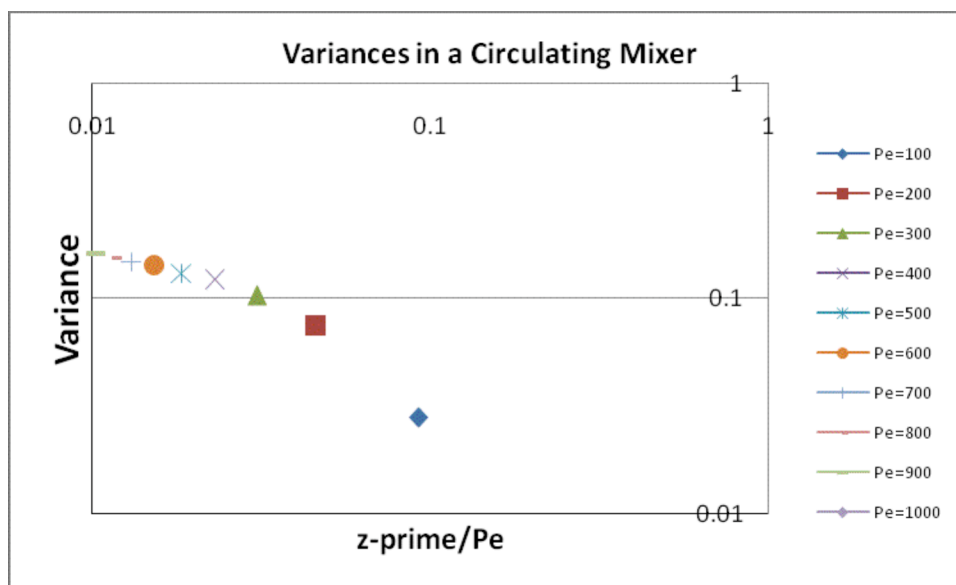


Figure 5: **Plotted Single 2D Mixer Variance with respect to Mixing Length & Pe Number.** This is the graph produced by plotting the variance versus the mixing path length over the Peclet number. For this scenario, the mixing path length was constant over one mixer. The same logarithmic trend from Fig 8.17 for the mixing variance of a T-sensor in the book Micro Instrumentation can be observed from the figure above [3].

z	Re	Pe	z/Pe	u	C mixing	C var
(cm)	D'Less	D'Less	(cm)	(m <sup>2</sup> /s)	(mol/(m*s))	(mol/(m*s))
9.19	1	100	0.0919	0.958	0.536	0.028
9.19	1	200	0.0459	0.958	0.536	0.075
9.19	1	300	0.0306	0.958	0.536	0.104
9.19	1	400	0.0230	0.958	0.535	0.123
9.19	1	500	0.0184	0.958	0.519	0.132
9.19	1	600	0.0153	0.958	0.519	0.142
9.19	1	700	0.0131	0.958	0.518	0.149
9.19	1	800	0.0115	0.958	0.517	0.155
9.19	1	900	0.0102	0.958	0.516	0.160
9.19	1	1000	0.0092	0.958	0.531	0.169

Table 2. **Solved parameters for a Single 2D Mixer for Varying Peclet Numbers.** This table contains the parameters obtained from varying the Peclet number from 100 to 1000 while maintaining a constant Reynolds number of 1. The flow velocity is observed to be consistently the same while mixing cup concentration displays insignificant differences. However, the mixing cup variances are shown to progressively increase.

Next examining the data generated for a four mixers in series, the following table contains the parameters determined while the Reynolds number was increased. Additional figures depicting the stream lines and colored concentration gradients are shown in the Additional Results section of the Appendix.

Re	Pe	_P	u	c_mixing	c_variance	x	c_optical	c_op_var	DOF	Elements
D'Less	D'Less	(N/m)	(m <sup>2</sup> /s)	(mol/(m*s))	(mol/(m*s))	(m <sup>2</sup> )	(mol/m <sup>2</sup> )	(mol/m <sup>2</sup> )		
10	1000	238	0.834	0.435	0.0378	30	0.0147	0.00817	77288	520
50	1000	403	0.958	0.455	0.0861	30	0.0152	0.0103	129353	520
100	1000	487	0.840	0.106	0.0123	30	0.00354	0.00103	77288	520
150	1000	653	0.844	0.156	0.0123	30	0.00522	0.00145	77288	520

Table 3. **Solved parameters for a 2D Mixers in Series for Varying Reynolds Numbers.** In comparison to a single mixer in 2D, mixing cup concentration does not seem to improve with additional mixers in series. In fact, mixing cup concentrations is observed to drastically decrease for Reynolds numbers 100 and 150 in comparison to 10 and 50.

Moving onto the 3D resulting obtained, the following table is used to determine the validity of 3D mixer simulations by comparing the mixing cup variances. The closer the mixing cup variances coincide for the three modeling scenarios, the more accurate the results generated since the 3D solutions with slip should be identical the 2D version.

	Re	Pe	u	Cmixing	C var	x	c_optical	c_op_var	DOF	Elements
	D'Less	D'Less	(m <sup>2</sup> /s)	(mol/(m*s))	(mol/(m*s))	(m <sup>2</sup> )	(mol/m)	(mol/m)		
<b>2-D</b>	1	1000	0.958	0.448	0.087	30	0.475	0.120	313319	10736
<b>3-D w/ Slip</b>	1	1000	0.958	0.456	0.044	30	0.015	0.008	67672	1326
<b>3-D w/out Slip</b>	1	1000	0.882	0.464	0.09662	30	0.0155	0.0067	67672	1326

Table 4. **Comparison of 2D and 3D Mixing Cup Variances for Mixers in Series.** The mixing cup variance of the 2D and 3D with slip exhibits a 50% difference, which indicates that the 3D solutions determined are not terribly accurate. This subsequently implies that the solution generated for the realistic conditions of 3D without slip at the top and bottom boundary walls is also should not be give a lot of credence.

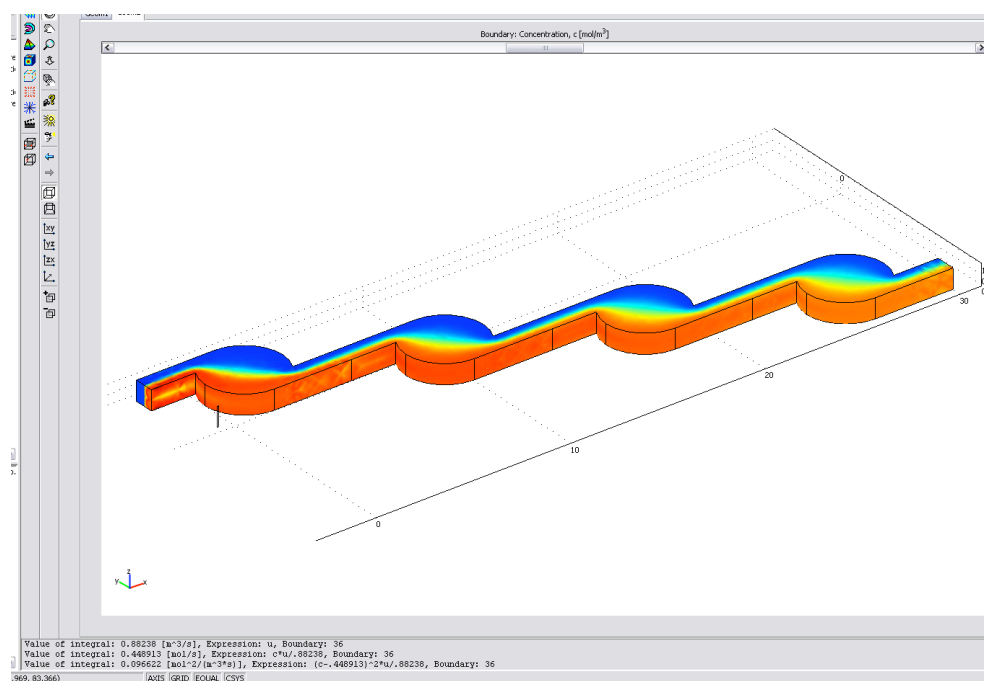


Figure 6: **3D Mixers with No Slip.** This is the 3D result generated by Comsol for no slip conditions with Re=1 and Pe=1000.

## Conclusions

First analyzing the 2D single mixer results presented above, the 2D variances presented for a single mixer collapse onto on curve as shown in Figure 5. Comparing the two figures, there are only two sets of Peclet numbers from the T-sensor variances that can be compared to the mixer. However, these sets of Peclet numbers do not correspond to the same  $z'/Pe$  region measured for the mixer. Then looking at mixing cup and optical variances, from Table 1, the values of each are consistently within the same order of magnitude and only differ by 14%. Of the two values the optical variance is consistently, this is important because some researchers use assess mixing by reading optical concentration using fluorescent markers in fluid which has a greater variance

than solving the Navier-Stokes equation for flow since the appearance of the markers is skewed on the varying velocities of the flow at different depths of vertical cross section boundary. Realizing this, it is important to ascertain the differences between these two approaches.

Also the varying the Reynolds number in an increasing fashion for a single mixer has the effect of increasing mixing cup concentration, having the best observed mixing for a  $Re=300$  and  $Pe=1000$  with a mixing cup concentration of  $0.75 \text{ mol/m}^2$ . Alternatively, increasing Reynolds number has the opposite for mixers in series, significantly lowering the mixing cup concentration in comparison for  $Re=100$  or  $150$  in comparison to  $Re=10$  or  $50$  in Table 3. Further explanation of this occurring phenomenon and suggestion to decrease mixing cup variance discussed in the Suggestion for Improved Mixing section. Whereas of the parameter observed while varying the Peclet number in a single mixer, only the mixing cup variance was significantly affected. From  $Pe=100$  to  $1000$ , the mixing cup variance was observed to increase from  $0.028$  to  $0.169 \text{ mol/m}^2$ .

Finally, comparing the results generated for a single mixer in 2D to those of the paper, the corresponding streamlines from Figure 4 are consistent and very similar to Figures 2 and 3 from the paper. This allows to conclude that the findings in the paper are reproducible and reasonable. Lastly, comparing the 2D to 3D results for mixers in series, Table 4 is used to determine the validity of 3D mixer simulations by comparing the mixing cup variances. The closer the mixing cup variances coincide for the three modeling scenarios, the more accurate the results generated since the 3D solutions with slip should be identical to the 2D version. The mixing cup variance of the 2D and 3D with slip exhibits a 50% difference, which indicates that the 3D solutions determined are not terribly accurate. This subsequently implies that the solution generated for the realistic conditions of 3D without slip at the top and bottom boundary walls is also should not be given a lot of credence.

## **Suggestions for Improved Mixing**

The best mixing seemed to be obtained using a single mixer at the highest Reynolds number of 300 where the mixing cup concentration is greatest at  $0.75 \text{ mol/m}^2$ . Oddly enough parameters recorded in Table 3 demonstrate that having several mixers in series actually lowered the mixing cup concentration for higher Reynolds numbers because the lower part of the stream initially containing high concentrations of solute is recirculated in the vortices of the mixers while the upper part of the stream containing no solution continues to flow directly through the mixers. Thus the circulating solution concentration is subsequently diluted with each vortex lowering the net mixing cup concentration with each pass through a mixer. These resulting stream profiles are displayed in the Additional Results section of the Appendix.

Also of all the scenarios modeled the lowest mixing cup variances generated were correlated with increased ratios of  $z'/Pe$ , meaning increased mixing length corresponding to decreased Peclet numbers. This can be observed when the mixing is increased to 4 times to original path

length of a single mixer to a series of four mixers which resulted in an order of magnitude reduction in mixing variance. For  $Re=10$  and  $Pe=1000$ , the mixing variance of a single mixer was  $0.169 \text{ mol/m}^2$  while for four mixers in series the mixing variance was  $0.01472 \text{ mol/m}^2$ .

## References

[1] Chung, Yung-Chiang, Yuh-Lih Hsu, Chun-Ping Jen, Ming-Chang Lu, and Yu-Cheng Lin. "Design of Passive Mixers Utilizing Microfluidic Self-Circulation in the Mixing Chamber." *Lab Chip* 4 (2004): 70-77. [RSC Publishing](#). UW Libraries, Seattle. 27 Mar. 2008. Keyword: Lab Chip.

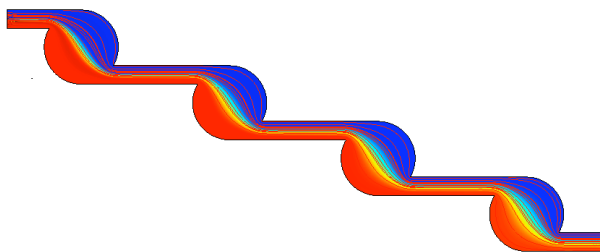
[2] Finlayson, Bruce A. *Introduction to Chemical Engineering Computing*. 1st ed. Hoboken: Wiley-Interscience, 2006. 201-202.

[3] Koch, Melvin V., Kurt M. VandenBussche, and Ray W. Chrisman, eds. *Micro Instrumentation for High Throughput Experimentation and Process Intensification - a Tool for PAT*. 1st ed. Wiley, 2007. 198-203.

## Appendix

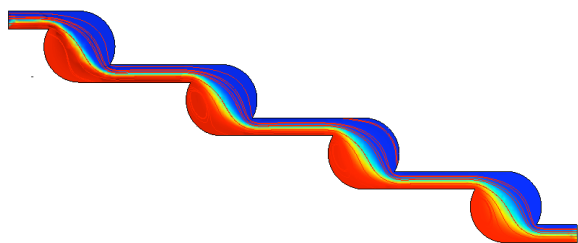
### 1. Additional Results

#### 2D Mixers in Series

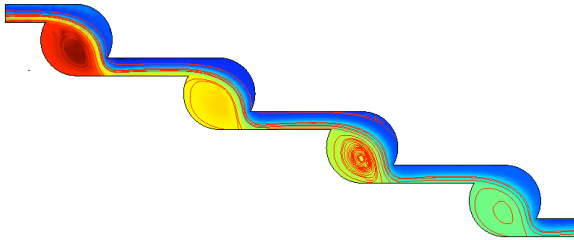


1.  $Re=1$

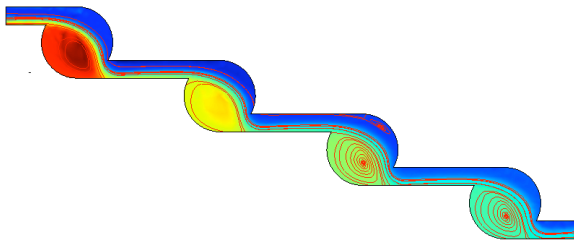
$Pe=1000$



2.  $Re=10$   
 $Pe=1000$



3.  $Re=100$   
 $Pe=1000$



4.  $Re=150$   
 $Pe=1000$

## 2. Sample Calculations

### Boundary Integrations

For  $Re=1$ ,  $Pe=1000$

### Mixing Cup Concentration

$$x\text{-velocity } (u) = .95833\text{m}^2/\text{s}$$

$$\int_A c \cdot u / 0.95833 = 0.530535 \text{ (mol/m}^2\text{)}$$

### Mixing Cup Concentration Variance

$$\int_A (c - 0.530535)^2 \cdot u / 0.95833 = 0.169115 \text{ (mol/m}^2\text{)}$$

### Optical Concentration

$$x = \text{integral path} = 30 \text{ m}^2$$

$$\int_A c / 30 = 0.5184 \text{ (mol/m}^2\text{)}$$

### Optical Concentration Variance

$$\int_A (c - 0.5184)^2 / 30 = 0.19592 \text{ (mol/m}^2\text{)}$$